Asia-Pacific Journal of Science and Technology: Volume: 31 Issue: 06 Article ID: APST-31-06-11 Research Article

APST

Asia-Pacific Journal of Science and Technology

https//:www.tci-thaijo.org/index.php/APST/index

Published by Research and Innovation Department,
Khon Kaen University, Thailand

Biosynthesis and Characterization of Bacteriocin-Capped Silver Nanoparticles and Their Antimicrobial Activity Against Pathogenic Bacteria

Intan Nur Sabrina Noor Azman[1], Wan Amirul Hakimi Wan Adnan[1], Sangkaran Pannerchelvan[1], Rosfarizan Mohamad[1,2], Nor'Aini Abdul Rahman[1,2], Helmi Wasoh[1,2,3], Mohamad Zulfazli Mohd Sobri[1,2] and Murni Halim[1,2,3]*

[1] Department of Bioprocess Technology, Faculty of Biotechnology and Biomolecular Sciences, Universiti Putra Malaysia, 43400, Serdang, Selangor, Malaysia.
[2] Bioprocessing and Biomanufacturing Research Centre, Universiti Putra Malaysia, UPM Putra Infoport – IOI Resort, 43400, Serdang, Selangor, Malaysia.
[3] Halal Products Research Institute, Universiti Putra Malaysia, 43400, Serdang, Selangor, Malaysia.
*Corresponding author: murnihalim@upm.edu.my

Received 4 February 2026
Revised 18 September 2026
Accepted 16 October 2026

Abstract

Antimicrobial resistance is an escalating global concern. Bacteriocins are promising antimicrobial peptides but are limited by proteolytic degradation and a narrow spectrum of activity. Conjugation of bacteriocins with silver nanoparticles (SNPs) can protect peptides and provide synergistic antimicrobial activity. This study reports the biosynthesis, optimization, physicochemical characterization and antibacterial evaluation of crude bacteriocin from *Lactiplantibacillus plantarum* strains T4 and B2, and commercially purified nisin, used to cap silver nanoparticles (Bac-SNPs and Nisin-SNPs). Optimal Bac-SNPs synthesis was achieved at Bacteriocin:$AgNO_3$ = 1:9 (v/v), 65°C and pH 11. UV-Vis spectroscopy showed surface plasmon resonance peaks between 400–500 nm, confirming SNPs formation. FTIR spectra indicated hydroxyl and carboxyl functional groups involved in capping. Dynamic light scattering revealed Z-average sizes of 63.14 nm (T4Bac-SNPs) and 80.65 nm (B2Bac-SNPs) with low polydispersity (PDI 0.260 and 0.263), whereas Nisin-SNPs exhibited larger hydrodynamic size (≈458 nm) and higher PDI (0.434), consistent with different capping behaviour. Antimicrobial evaluation demonstrated that Nisin-SNPs enhanced the activity of purified nisin against all tested pathogens (*Listeria monocytogenes*, *Bacillus cereus* and *Escherichia coli*), with the most prominent inhibition observed against *E. coli* (18.00 ± 0.00 mm). In contrast, Bac-SNPs derived from strains T4 and B2 showed lower or comparable inhibition zones relative to their corresponding crude bacteriocins, indicating that nanoparticles conjugation did not uniformly enhance antibacterial activity. Overall, the findings demonstrate that bacteriocin type and synthesis conditions critically influence the physicochemical properties and antibacterial performance of bacteriocin-capped silver nanoparticles.

Keywords: Antimicrobial resistance, Bacteriocin, Bacteriocin-capped silver nanoparticles, *Lactiplantibacillus plantarum*, Nisin-capped silver nanoparticles

1. Introduction

Antimicrobial resistance (AMR) is a growing global concern that threatens public health, food safety, and clinical treatment efficacy. The widespread and often indiscriminate use of antibiotics has accelerated the emergence of resistant bacterial strains, reducing the effectiveness of conventional antimicrobial therapies. As a result, there is an urgent need to develop alternative antimicrobial strategies that are effective, sustainable, and less prone to resistance development [1].

Bacteriocins are ribosomally synthesized antimicrobial peptides produced by bacteria, particularly lactic acid bacteria (LAB). These peptides exhibit strong antimicrobial activity, primarily against closely related bacterial

species, and are generally recognized as safe due to their proteinaceous nature and biodegradability. Bacteriocins exert their antimicrobial effects through diverse mechanisms, such as forming pores in the cytoplasmic membrane, causing leakage of cellular contents and eventual cell death, or interfering with essential cellular processes like cell wall synthesis or protein synthesis [2,3]. Among bacteriocins, nisin produced by *Lactococcus lactis* is one of the most extensively studied and commercially applied bacteriocins, widely used as a food preservative [4,5].

Despite their advantages, bacteriocins have limitations that restrict their broader application. These include susceptibility to enzymatic degradation, reduced stability under extreme pH or temperature conditions, limited antimicrobial spectrum, and reduced efficacy against Gram-negative bacteria due to the presence of an outer membrane [6]. Consequently, strategies to enhance the stability, spectrum, and antimicrobial efficacy of bacteriocins are actively being explored.

Nanotechnology has emerged as a promising approach to address these limitations. Metallic nanomaterials such as silver nanoparticles (SNPs) and gold nanoparticles (AuNPs) exhibit unique surface plasmon resonance (SPR), high surface-are-to-volume ratios, and tuneable surface chemistry [7]. However, several key differences in reactivity, oxidation behaviour, biocidal activity and economic viability distinguish AgNPs from AuNPs and make AgNPs preferable for certain practical applications. The sustained release of bioactive silver ions contributes to the broad-spectrum antimicrobial activity of AgNPs, whereas intact AuNPs generally require external functionalization or high dosages to achieve comparable biocidal activity [8]. AgNPs also exhibit stronger and sharper SPR absorption bands, resulting in more pronounced visual colour transitions than those of AuNPs [9]. Their high molar extinction coefficient makes AgNPs highly sensitive for colorimetric detection, making them potentially suitable for smart or indicator packaging applications. In addition, AgNPs provide greater electromagnetic field enhancement than AuNPs, making them more suitable for surface-enhanced Raman scattering (SERS)-based sensor platforms for the sensitive detection of foodborne pathogens, mycotoxins and pesticide residues [10]. Furthermore, silver is substantially less expensive than gold as a raw material, thereby facilitating scalable commercial production of AgNP-based technologies [11].

SNPs are of particular interest due to their broad-spectrum antimicrobial activity and multiple mechanisms of action, including disruption of bacterial cell membranes, generation of reactive oxygen species, interference with DNA replication, and inhibition of essential enzymes [12]. These multiple modes of action reduce the likelihood of resistance development and make SNPs effective against both Gram-positive and Gram-negative bacteria. The conjugation of bacteriocins with silver nanoparticles represents a synergistic antimicrobial strategy that combines the specificity of bacteriocins with the broad-spectrum activity of SNPs. Bacteriocins can act as reducing and stabilizing agents during nanoparticle synthesis, enabling environmentally friendly biosynthesis while potentially improving peptide stability and bioavailability. Numerous studies have demonstrated the efficacy of Bac-SNPs against a wide range of multidrug-resistant bacterial pathogens, including methicillin-resistant *Staphylococcus aureus* [13]. However, the extent of enhancement depends on bacteriocin purity, synthesis conditions, and nanoparticle characteristics.

In this study, Bac-SNPs were biosynthesized using crude bacteriocin produced by *L. plantarum* strains T4 and B2, as well as commercially purified nisin. The synthesis conditions were optimized, and the nanoparticles were characterized using UV-Vis spectroscopy, Fourier-transform infrared spectroscopy (FTIR), and dynamic light scattering (DLS). To evaluate the broad-spectrum antibacterial potential of Bac-SNPs and Nisin-SNPs, *L. monocytogenes* and *B. cereus* were selected as representative Gram-positive foodborne pathogens, while *E. coli* was chosen as a representative Gram-negative pathogen due to their high prevalence in fresh produce contamination and major importance to food safety and public health [14]. Furthermore, Sidhu and Nehra [6] reported that Bac-SNPs synthesised using the bacteriocins Bac4463 and Bac22 exhibited significant inhibitory activity against *L. monocytogenes*, *E. coli*, and *B. cereus*, among others. The antimicrobial activity of these nanoconjugates was found to be superior to that of their individual components, suggesting a synergistic effect. This work provides insight into the comparative performance of crude bacteriocin-based and purified bacteriocin-based nanoparticle systems and their potential applications as alternative antimicrobial agents.

2. Materials and Methods

2.1 Microorganisms and culture conditions

L. plantarum strains T4 and B2 were used as bacteriocin-producing strains. The strains were maintained on de Man, Rogosa and Sharpe (MRS) agar and cultured in MRS broth (Oxoid LTD, Basingstoke, Hampshire, GB) at 37°C with agitation at 150 rpm (Lab Companion IS-971R Incubated Laboratory Shaker, JEIO TECH, Korea). Indicator pathogenic bacteria like *L. monocytogenes*, *B.cereus*, and *E. coli* (obtained from Microbial Culture Collection Unit (UNiCC) at UPM) were maintained on nutrient agar and cultured in nutrient broth (Oxoid LTD, Basingstoke, Hampshire, GB) under aerobic conditions at 37°C (Memmert INE600 Incubator, Memmert GmbH, Germany) prior to use.

2.2 Production and preparation of bacteriocin

Active cultures of both *L. plantarum* T4 and B2 were inoculated into the MRS broth and incubated at 37°C at 150 rpm for 14 hours. After incubation, the supernatants were collected by centrifuging the grown cultures at 10,000 rpm for 15 minutes at 4°C (Microfuge 16, Benchtop Centrifuge, Beckman Coulter, USA). To neutralize the effect of organic acids in the collected supernatants, the pH was adjusted to 6.0 (Eutech™ pH 700 Meter, Thermo Scientific Eutech, Singapore) using a 1N sodium hydroxide (NaOH) (R&M Chemicals, Malaysia) solution, and the neutralized supernatants were then filtered using a 0.22 µm membrane filter.

2.3 Biosynthesis of bacteriocin-capped silver nanoparticles (Bac-SNPs)

Silver nanoparticles were synthesized using bacteriocin as both reducing and stabilizing agents according to the method described by Sidhu and Nehra with slight modifications [6]. A 2 mM solution of silver nitrate ($AgNO_3$) (System Chemicals, Malaysia) was prepared with continuous stirring for 5–6 hours on a magnetic stirrer at room temperature (Stirring hotplate FAVORIT ®, PLT Scientific, Malaysia). An aliquot of 5 mL of the crude bacteriocin obtained from *L. plantarum* T4 and B2 was separately added to 45 mL of freshly prepared 2 mM $AgNO_3$ solution. The resultant mixed solution was incubated under UV light for 50–60 minutes at room temperature (ERLA CFM-4 Laminar Air Flow, ERLA Technologies, Malaysia). A change in colour from light yellow to reddish-brown indicated the formation of SNPs. The obtained suspension was then centrifuged at 15,000 rpm for 20 minutes (Avanti J-26 XPI High-Performance Centrifuge, Beckman Coulter, USA) to pellet the Bac-SNPs, which were subsequently washed three times with distilled water to remove unbound $AgNO_3$ and free bacteriocins.

2.4 Biosynthesis of nisin-capped silver nanoparticles (Nisin-SNPs)

For Nisin-SNPs synthesis, 10 mg of commercial nisin (Glentham Life Sciences, UK) was dissolved and mixed with 10 mL of 1 mM $AgNO_3$ solution [15]. The mixture was incubated at room temperature in the dark under constant stirring at 150 rpm for 24 hours. The resulting suspension was centrifuged at 3,500 rpm for 20 minutes, and the pellet was washed twice with phosphate-buffered saline (PBS) (1st BASE, Singapore) to remove excess reagents. The final suspension was stored at 4°C.

2.5 Optimization of synthesis parameters

Optimization of Bac-SNPs synthesis was conducted by varying Bacteriocin:$AgNO_3$ ratios (0.5:9.5, 1:9, 1.5:8.5, and 2:8 v/v), temperature (35–75°C), and pH (3–13). Optimal conditions were selected based on intensity of surface plasmon resonance (SPR) peaks, stability of the nanoparticle suspension, and preliminary antimicrobial activity.

2.6 Characterization of nanoparticles

UV-Vis spectroscopy (SP-V1000 Spectrophotometer, DLAB Scientific, China) was used to confirm nanoparticle formation by scanning samples between 300–700 nm. Functional groups involved in nanoparticle capping were identified using Fourier-transform infrared spectroscopy (FTIR) (Spectrum 3 Tri-Range FT-IR Spectrometer, PerkinElmer, USA) in the range of 4000–400 cm^{-1}. Particle size distribution and polydispersity index (PDI) were measured using dynamic light scattering (DLS) (Zetasizer Nano S ZEN1600, Malvern Panalytical, UK).

2.7 Antibacterial activity assay

The antibacterial activity of crude bacteriocin (T4 and B2), Bac-SNPs (T4Bac-SNPs and B2Bac-SNPs), Nisin, and Nisin-SNPs against *L. monocytogenes, B. cereus*, and *E. coli* was evaluated by using agar well diffusion method. Overnight grown pathogen cultures were prepared and adjusted to a turbidity equivalent to the 0.5 McFarland (1.5×10^8 CFU/mL). Subsequently, 100 µL of the bacterial suspension was evenly spread onto the surface of Mueller-Hinton agar (MHA) (Oxoid LTD, Basingstoke, Hamsphire, UK). The test sample and control sample (positive control, 10 µg ampicillin and negative control, MRS broth without cell) were placed on the separated well (8mm) prepared priorly on lawned cultured MHA and incubated at 37°C for 24 h. A clear zone around the well indicates a positive result, in which the diameter of the inhibition zone was measured in millimeters (mm).

2.8 Statistical Analysis

All assays were performed in triplicate, and results were expressed as mean ± standard deviation. Statistical significance was evaluated using the Student's t-test, with a significance threshold set at $P > 0.05$.

3. Results

3.1 Visual observation and optimization of nanoparticle synthesis

Bacteriocin-mediated synthesis of silver nanoparticles was confirmed by a colour change from pale yellow to reddish-brown after UV exposure (Figure 1). Reaction mixtures containing crude bacteriocin from *L. plantarum* T4 and B2 (T4Bac-SNPs and B2Bac-SNPs) developed the characteristic brown coloration, indicating reduction of Ag^{+} to Ag^{0} and formation of silver nanoparticles due to SPR [16]. The consistent colour intensity suggests the nanoparticles were stable and predominantly spherical.

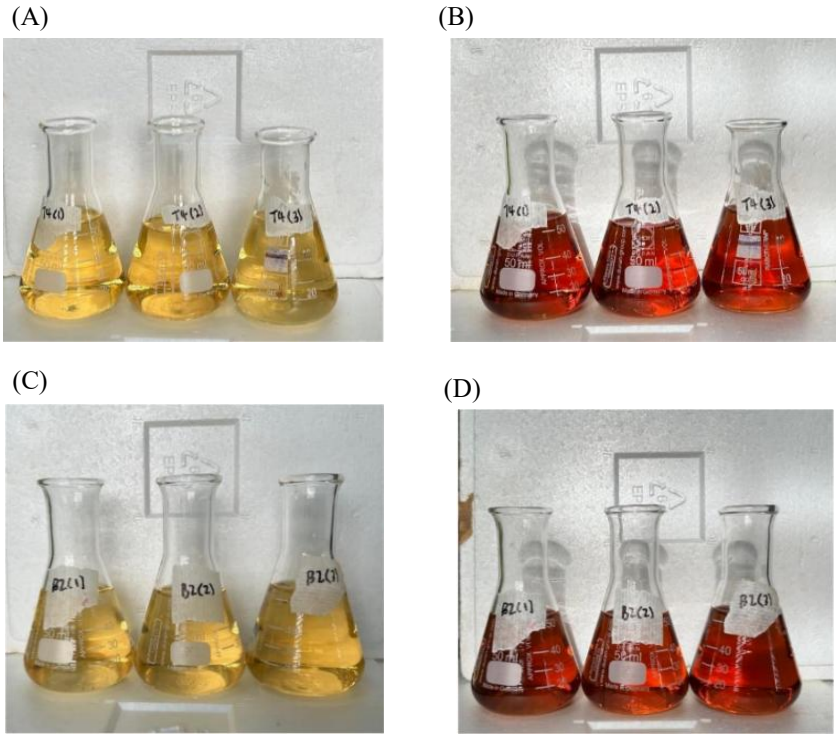


Figure 1 Colour observation of the synthesised of Bac-SNPs. Images (A) Crude bacteriocin of *L.plantarum* T4 and (C) Crude bacteriocin of *L. plantarum* B2 show the pale-yellow coloration of the reaction mixtures prior to UV light exposure. Images (B) and (D) display the distinct reddish-brown coloration of the mixtures after UV exposure for Crude bacteriocin of *L. plantarum* T4 and B2, respectively.

3.2 Optimisation of Bac-SNPs under Different Synthesis Conditions

Optimization of Bac-SNPs synthesis was evaluated by UV–Vis spectroscopy based on SPR within 400–500 nm. Nanoparticle formation was observed under all tested bacteriocin concentrations, temperatures, and pH conditions, but SPR intensity and peak sharpness varied. The optimal Bacteriocin-to-$AgNO_3$ ratio was 1:9, producing the highest and sharpest SPR peaks (420–430 nm) for both T4Bac-SNPs and B2Bac-SNPs, while lower or higher ratios resulted in reduced absorbance or peak broadening (Figure 2). Temperature strongly influenced synthesis, with maximal SPR intensity at 65°C (420 nm) for both strains, whereas lower temperatures produced weak or broad peaks and 75°C caused slight declines in absorbance (Figure 3).

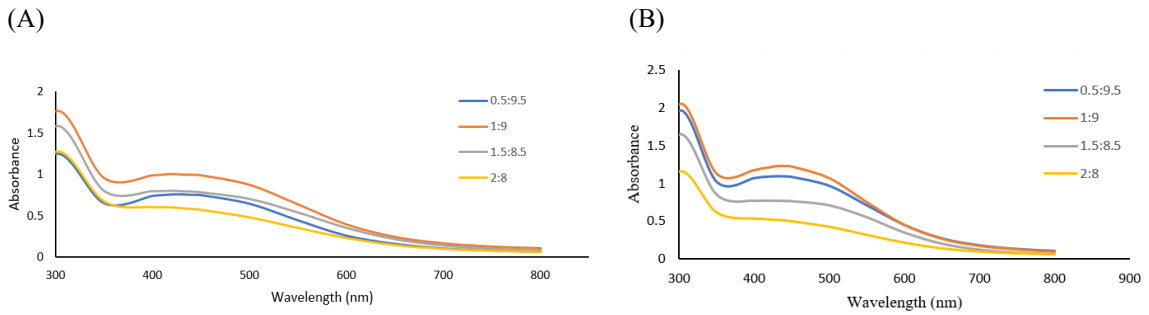


Figure 2 Absorbance spectra from UV-Vis Spectroscopy for Bac-SNPs samples synthesised at different bacteriocin concentration (0.5:9.5, 1:9, 1.5:8.5, and 2:8), in mL, using: (A) Crude bacteriocin of *L. plantarum* T4; and (B) Crude bacteriocin of *L. plantarum* B2, at room temperature, pH 6 for 24 hours.

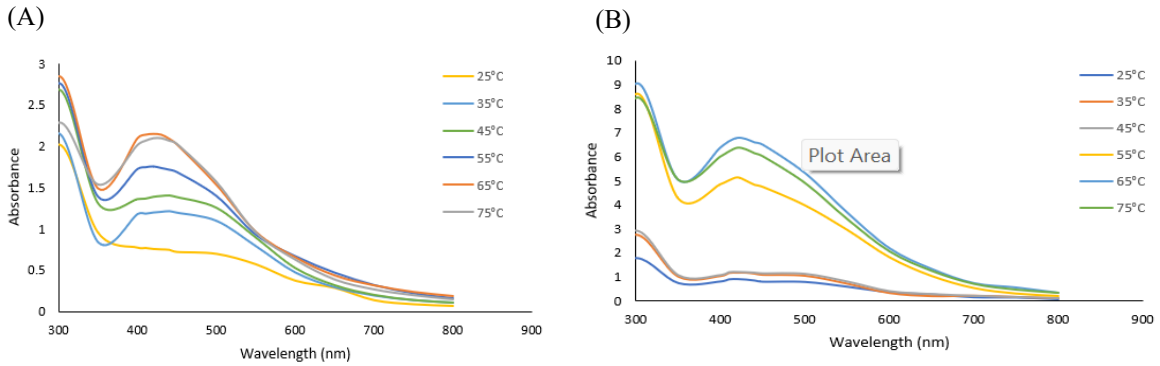


Figure 3 Absorbance spectra from UV-Vis Spectroscopy for Bac-SNPs samples synthesised at different temperature (25°C, 35°C, 45°C, 55°C, 65°C, and 75°C), using: (A) Crude bacteriocin of *L. plantarum* T4; and (B) Crude bacteriocin of *L. plantarum* B2, with the concentration ratio of 1:9 (mL) and neutral pH for 24 hours.

Similarly, pH strongly influenced synthesis, with no distinct SPR peaks at pH 3, indicating poor reduction under acidic conditions (Figure 4). While progressively sharper and more intense peaks were observed from pH 5 to alkaline conditions (pH 9–13), demonstrating enhanced nanoparticle formation and stability. Alkaline pH also favoured more uniform nanoparticle morphology compared to acidic conditions [17]. Overall, a bacteriocin ratio of 1:9, temperature of 65°C, and alkaline pH provided the most efficient Bac-SNPs synthesis.

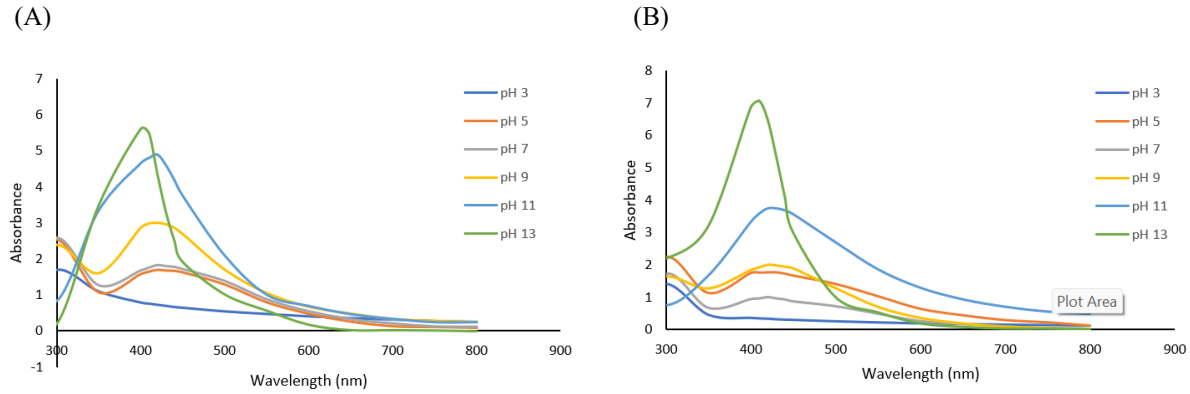


Figure 4 Absorbance spectra from UV-Vis Spectroscopy for Bac-SNPs samples synthesised at different pH (pH 3, pH 5, pH 7, pH 9, pH 11, and pH 13), using: (A) Crude bacteriocin of *L. plantarum* T4; and (B) Crude bacteriocin of *L. plantarum* B2, with the concentration ratio of 1:9 (mL) at 65°C for 24 hours.

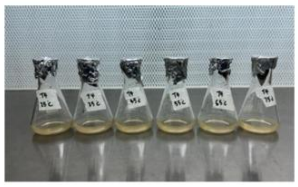
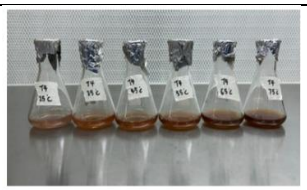
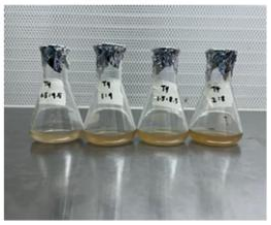
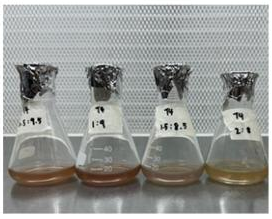
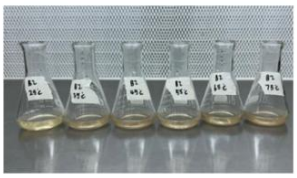
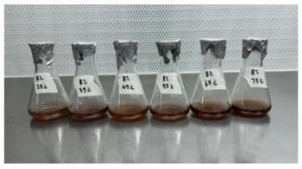
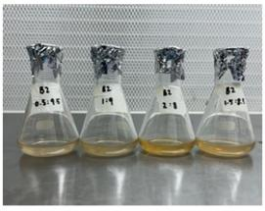
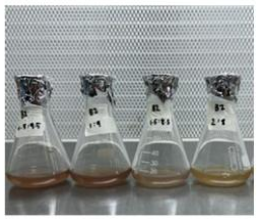
3.3 Screening of Optimal Conditions for Bac-SNPs Activity

The optimization process for Bac-SNPs was conducted under controlled conditions, focusing on the three critical factors: bacteriocin concentration (1:9 mL), temperature (65°C), and pH. For bacteriocin concentration

and temperature, visual observation during the synthesis showed a characteristic reddish-brown coloration (Table 1), indicating successful SNPs formation.

Upon observation, SNPs at pH 13 appeared darker in colour compared to those synthesized at lower pH levels (Figure 5). Therefore, to evaluate whether high pH influences the antimicrobial activity, SNPs synthesized at pH 13 were subjected to agar well diffusion assays alongside those prepared at pH 11 as a preliminary step. The results showed that SNPs at pH 13 showed no inhibition zones for both T4Bac-SNPs and B2Bac-SNPs, highlighting a significant reduction in antimicrobial efficacy compared to the observable inhibition zones at pH 11 (Table 2).

Table 1 The colour observation of the synthesised Bac-SNPs (T4Bac-SNPs and B2Bac-SNPs) (A) at different temperature and (B) different concentration.

(A)		(B)	
Before reaction	After reaction	Before reaction	After reaction
			
T4-SNPs	T4-SNPs	T4-SNPs	T4-SNPs
			
B2-SNPs	B2-SNPs	B2-SNPs	B2-SNPs

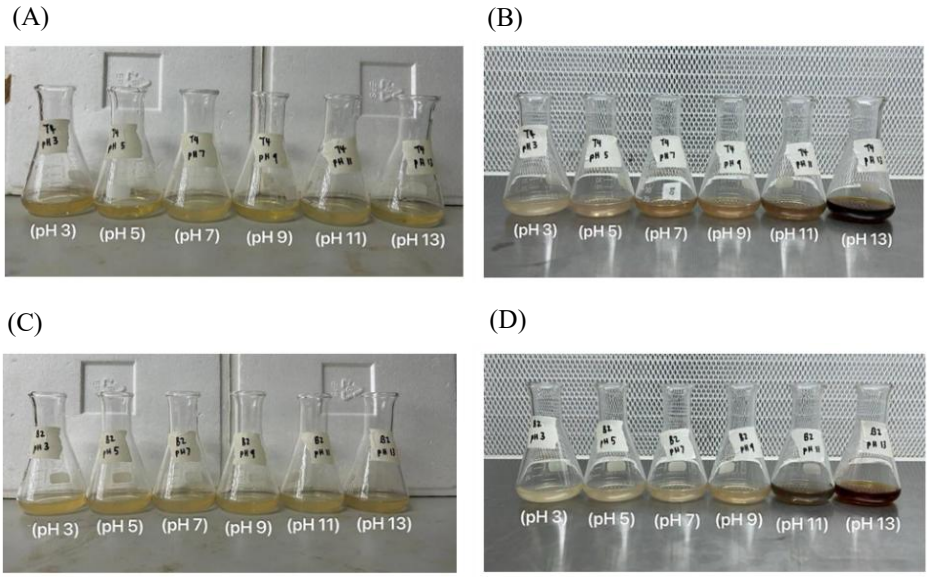


Figure 5 Colour observation of Bac-SNPs under varying pH conditions (pH 3, 5, 7, 9, 11, and 13) at an optimized concentration ratio of 1:9 (mL) and a temperature of 65°C. Images illustrate the colour of Bac-SNPs solutions: (A) T4Bac-SNPs before reaction; (B) T4Bac-SNPs after reaction; (C) B2Bac-SNPs before reaction; and (D) B2Bac-SNPs after reaction.

Table 2 Effect of pH conditions on the antibacterial activity of T4Bac-SNPs and B2Bac-SNPs against *L. monocytogenes*

Sample	Mean zone of inhibition (mm) ± SD	
	pH 11	pH 13
T4Bac-SNPs	11.00 ± 0.00	0
B2Bac-SNPs	12.00 ± 0.00	0

To address this limitation, pH 11 was evaluated as a more suitable condition for antimicrobial testing. The SNPs synthesized at pH 11 retained their colloidal stability and exhibited observable inhibition zones, measuring 11.00 mm for T4Bac-SNPs and 12.00 mm for B2Bac-SNPs against *L. monocytogenes.* The lighter colour of SNPs solutions at pH 11 corroborates the absence of significant aggregation, thereby confirming the formation of stable SNPs suspensions. Based on these findings, pH 11 was selected as the optimized pH condition, alongside a Bacteriocin:$AgNO_3$ ratio of 1:9 and a synthesis temperature of 65°C. These optimized parameters were then used for subsequent characterization studies.

3.4 Characterization of Bac-SNPs

Bac-SNPs synthesized under optimized conditions (Bacteriocin:$AgNO_3$ 1:9, 65 °C, pH 11) was characterized by UV–Vis, FTIR, and DLS. UV-Vis spectroscopy revealed characteristic surface plasmon resonance (SPR) peaks between 415 and 416 nm for both Bac-SNPs, confirming silver nanoparticle formation (Figure 6). Variations in peak intensity and width were observed depending on synthesis conditions, suggesting differences in particle size distribution and aggregation behaviour.

FTIR spectra of T4Bac-SNPs and B2Bac-SNPs exhibited absorption bands corresponding to O–H and N–H stretching vibrations, amide I and II bands, and C=O stretching (Figure 7). These functional groups indicate the involvement of peptide bonds and hydroxyl groups in the reduction and stabilization of silver nanoparticles (Table 3). DLS analysis showed that Bac-SNPs synthesized from *L. plantarum* T4 and B2 had Z-average diameters of 63.14 nm and 80.65 nm, respectively, with low polydispersity indices (<0.30) (Figure 8).

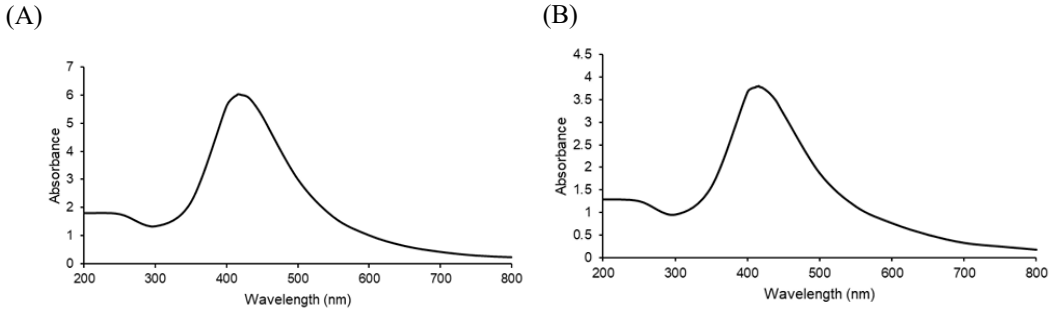


Figure 6 Absorbance spectra from UV-Vis Spectroscopy for Bac-SNPs synthesised at optimised condition (concentration ratio of 1:9 mL, 65°C, and pH 11): (A) T4Bac-SNPs and (B) B2Bac-SNPs.

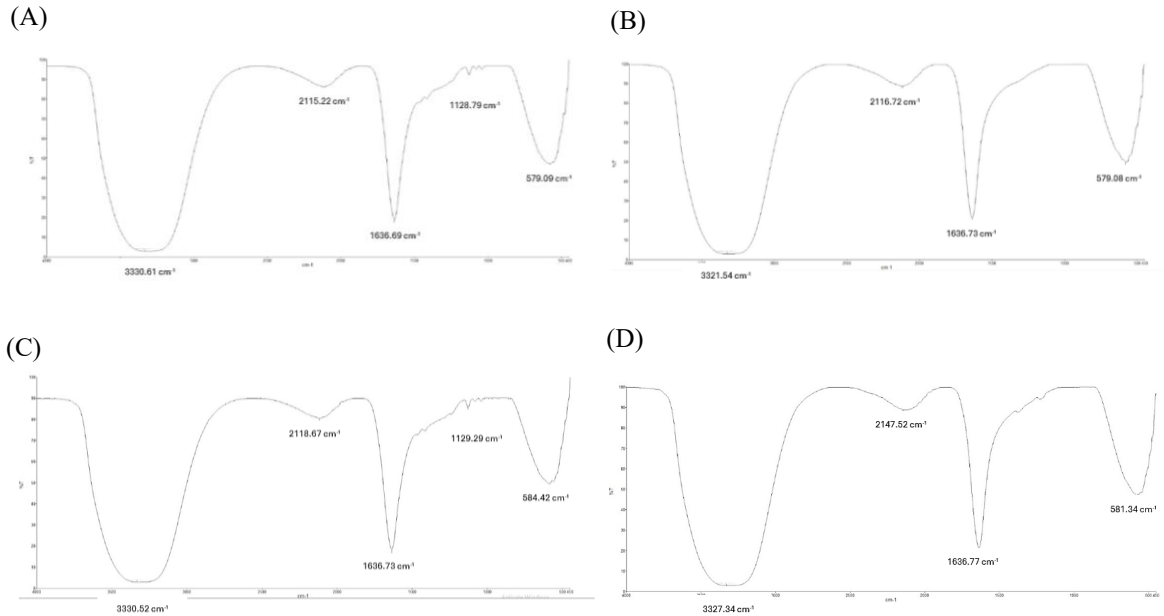


Figure 7 FTIR spectra peak for: (A) Crude bacteriocin T4; (B) T4Bac-SNPs; (C) Crude bacteriocin B2; (D) B2Bac-SNPs within the range of 4000 cm^{-1} to 400 cm^{-1}.

Table 3 The peak number and their respective positions of wavenumber (cm-1) for FTIR spectroscopy of T4Bac-SNPs, B2Bac-SNPs, and SNPs (from published reports).

Peak no.	Functional groups	FTIR wavenumber (cm^{-1})				
		T4Bac-SNPs	B2Bac-SNPs	[a]SNPs	[b]SNPs	[c]SNPs
1	Fingerprint region	579.08	581.34	-	-	-
2	C-O/C-N	-	-	1212.28	1217.03	1255.67
3	C-H	-	-	1366.08	1365.57	1434.23
4	Amide I	1636.73	1636.77	1639.04	1638.64	1636.95
5	C≡C/C≡N	2116.72	2147.52	2134.19	2140.14	2159.00
6	O-H/N-H	3321.54	3327.34	3354.84	3354.07	3339.49

Notes: [a][18], [b] [6], [c][19]

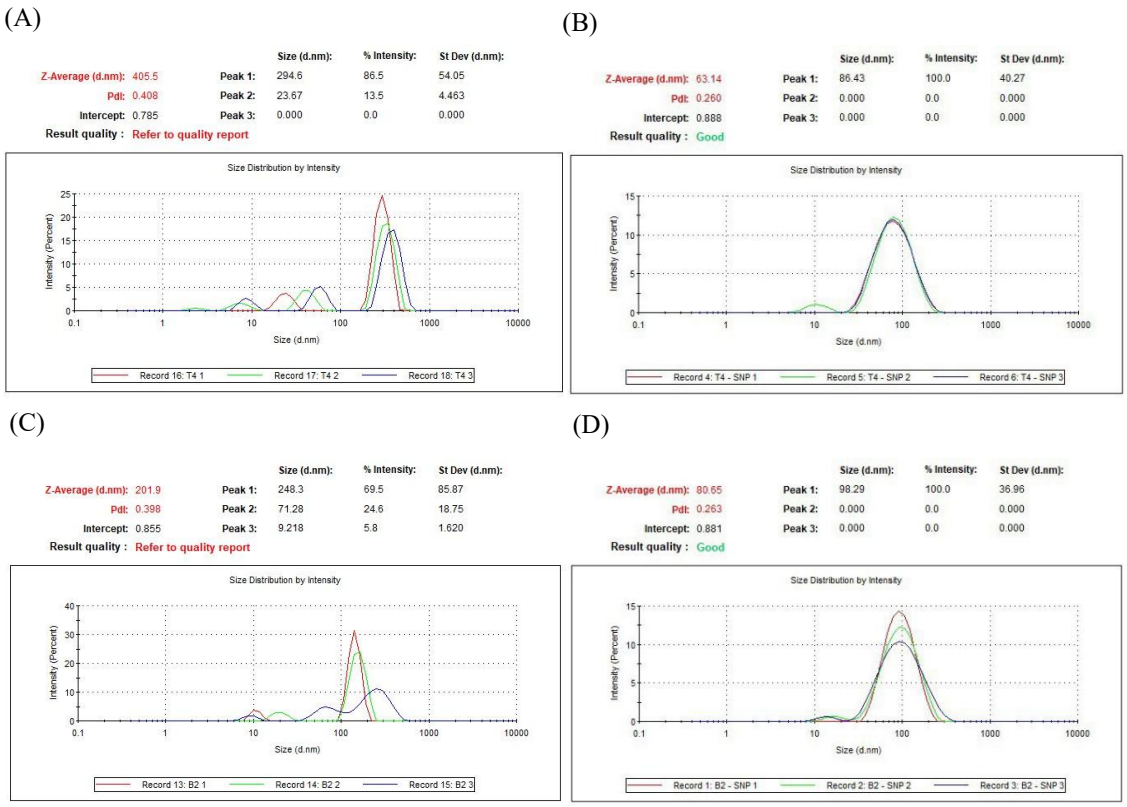


Figure 8 DLS analysis for the determination of the Z-average and PDI of: (A) Crude bacteriocin T4; (B) T4Bac-SNPs; (C) Crude bacteriocin B2; (D) B2Bac-SNPs.

3.5 Antibacterial activity

The antibacterial activity of crude bacteriocin (T4 and B2), Bac-SNPs (T4Bac-SNPs and B2Bac-SNPs), Nisin, and Nisin-SNPs against *L. monocytogenes, B. cereus*, and *E. coli* was evaluated by the measurement of the inhibition zones. The results show distinct patterns of antibacterial efficacy influenced by the molecular composition, synthesis method, and potential synergistic effects. The inhibition zones for crude bacteriocin T4 and B2 were notably larger compared to their respective SNP-conjugated forms (T4Bac-SNPs and B2Bac-SNPs) as shown in Table 4. Against *L. monocytogenes*, the inhibition zones were 12.67 ± 0.58 mm (T4) and 13.33 ± 0.58 mm (B2), compared to the reduced zones of 11.00 ± 0 mm and 12.00 ± 0 mm for T4Bac-SNPs and B2Bac-SNPs, respectively. A similar trend was observed against *B. cereus* and *E. coli*.

In contrast, Nisin-SNPs exhibited significantly greater antibacterial activity compared to pure nisin (Table 5), showing inhibition zones of 15.00 ± 0 mm (*L. monocytogenes*), 14.5 ± 0.71 mm (*B. cereus*), and 18.00 ± 0 mm (*E. coli*), as opposed to 11.33 ± 0.58 mm, 10.00 ± 0 mm, and 11.00 ± 0 mm for nisin alone.

Table 4 Antibacterial activity analysis for crude bacteriocin (T4 and B2) and Bac-SNPs (T4Bac-SNPs and B2Bac-SNPs) against three pathogenic bacterial strains

Bacterial strains	Mean of inhibition zone (mm) ± SD			
	Crude bacteriocin T4	T4Bac-SNPs	Crude bacteriocin B2	B2Bac-SNPs
L. monocytogenes	$12.67^{a} \pm 0.58$	$11.00^{b} \pm 0.00$	$13.33^{a} \pm 0.58$	$12.00^{b} \pm 0.00$
B. cereus	$16.00^{a} \pm 0.00$	$11.00^{b} \pm 0.00$	$16.67^{a} \pm 0.58$	$11.00^{b} \pm 0.00$
E. coli	$16.33^{a} \pm 0.58$	$11.00^{b} \pm 0.00$	$16.67^{a} \pm 0.58$	$11.00^{b} \pm 0.00$

Notes: Different letters (a and b) in the same row (Crude bacteriocin T4 and T4Bac-SNPs; Crude bacteriocin B2 and B2Bac-SNPs) are significantly different ($p < 0.5$).

Table 5 Antibacterial activity analysis for pure nisin and Nisin-SNPs against three pathogenic bacterial strains

Bacterial strains	Mean of inhibition zone (mm) ± SD	
	Nisin	Nisin-SNPs
L. monocytogenes	$11.33^{b} \pm 0.58$	$15.00^{a} \pm 0.00$
B. cereus	$10.00^{b} \pm 0.00$	$14.50^{a} \pm 0.71$
E. coli	$11.00^{b} \pm 0.00$	$18.00^{a} \pm 0.00$

Notes: Different letters (a and b) in the same row are significantly different ($p < 0.5$)

4. Discussion

The biosynthesis of Bac-SNPs represents an innovative approach to harnessing the antimicrobial potential of silver nanoparticles stabilized and reduced by bacteriocin. This process leverages the dual functionality of bacteriocin molecules as both reducing agents for silver ions (Ag^{+}) and capping agents for stabilizing nanoparticles [20]. The synthesis of Bac-SNPs was systematically optimized by evaluating the effects of bacteriocin concentration, temperature, and pH, with nanoparticle formation verified through UV–Vis detection of surface plasmon resonance (SPR) within 400–500 nm [2,21]. Variation in bacteriocin concentration demonstrated that a Bacteriocin:$AgNO_3$ ratio of 1:9 produced the most intense and well-defined SPR peak, indicating an optimal balance between Ag^{+} reduction and nanoparticle stabilization, whereas higher concentrations reduced spectral intensity and peak sharpness, suggesting oversaturation and particle aggregation [22,23,24]. Temperature significantly influenced reaction kinetics, with weak and broad SPR peaks observed at lower temperatures due to limited reduction efficiency, while synthesis at 65 °C yielded the highest absorbance and sharpest SPR signals, reflecting enhanced nanoparticle yield and uniformity; further temperature increase led to a slight decline in intensity, likely due to partial degradation of bacteriocin biomolecules [17]. Similarly, pH strongly affected nanoparticle formation, as acidic conditions suppressed SPR development, whereas alkaline environments (pH 9–13) produced the most pronounced and narrow SPR peaks, consistent with improved reduction kinetics, stronger electrostatic stabilization, and formation of predominantly uniform nanoparticles [25]. While the initial characterization indicated that pH 13 exhibited the highest SPR peak and a darker colour than the samples prepared at lower pH values (pH 11 and below) (Figure 4), the corresponding antimicrobial assay showed no detectable inhibition zone. This finding suggests that a stronger SPR response does not necessarily correspond to enhanced antimicrobial activity [26]. The absence of an inhibition zone at pH 13 may be attributed to changes in silver speciation and reduced bioavailability of antimicrobial Ag^{+} species under highly alkaline conditions, specifically the precipitation or formation of insoluble silver oxides and hydroxides, which limit free active silver ions [27]. Furthermore, extreme alkaline conditions alter nanoparticle surface chemistry, capping agent charge, and aggregation dynamics, which could limit the diffusion of nanoparticles through the agar matrix and inhibit their physical interation with bacterial cell walls [27,28].

Characterization of Bac-SNPs synthesized under optimized conditions (Bacteriocin:$AgNO_3$ = 1:9, 65 °C, pH 11) and Nisin-SNPs prepared using baseline parameters confirmed successful nanoparticle formation and biomolecule-mediated stabilization. UV–Vis spectroscopy revealed distinct SPR peaks within 400–450 nm for T4Bac-SNPs (416 nm), B2Bac-SNPs (415 nm), and Nisin-SNPs (400 nm), indicating predominantly spherical, well-dispersed silver nanoparticles with good colloidal stability [15]. FTIR spectra demonstrated shifts and intensity changes in functional group bands (notably O–H/N–H, C=O amide I, and C≡N/C≡C), confirming the involvement of proteins and peptides in reduction and capping of SNPs through coordination with silver ions [29]. DLS analysis further supported nanoparticle formation, showing substantial reductions in hydrodynamic size and polydispersity for Bac-SNPs compared to their parent bacteriocin solutions, indicating improved uniformity and dispersion [22,30]. In contrast, Nisin-SNPs exhibited a larger hydrodynamic diameter and slightly higher PDI than pure nisin, suggesting nanoparticle–peptide conjugation that increased apparent particle size, consistent with previous reports [31]. Collectively, these findings verify that bacteriocin functioned effectively as reducing and stabilizing agents, producing stable silver nanoparticles with distinct physicochemical characteristics.

Antibacterial assays demonstrated contrasting effects of nanoparticle conjugation on bacteriocin and nisin. Crude bacteriocin (T4 and B2) produced larger inhibition zones than their corresponding Bac-SNPs against *L. monocytogenes*, *B. cereus*, and *E. coli*, suggesting that bioactive metabolites present in the cell-free supernatant, such as organic acids and hydrogen peroxide, may have contributed synergistically to antimicrobial activity

[32,33]. Variability in crude bacteriocin composition and the dilution of active bacteriocin components during nanoparticle synthesis may have reduced the apparent efficacy of Bac-SNPs, highlighting the importance of purification and concentration standardization [34]. In contrast, Nisin-SNPs exhibited markedly enhanced antibacterial activity compared with free nisin, producing substantially larger inhibition zones against all tested pathogens, which may be attributed to the intrinsic antimicrobial properties of silver nanoparticles and their ability to intensify membrane disruption and oxidative stress, thereby potentiating nisin activity [12]. The use of controlled concentrations during Nisin-SNPs synthesis likely further contributed to the consistency and enhanced efficacy observed. Collectively, these findings indicate that while nanoparticle conjugation may reduce the apparent activity of crude bacteriocin due to compositional and dilution effects, it can significantly enhance the antimicrobial performance of purified bacteriocins such as nisin through synergistic nano–bio interactions.

5. Conclusion

Bacteriocin-capped silver nanoparticles were successfully biosynthesized and characterized. Optimized Bac-SNPs (Bacteriocin:$AgNO_3$ 1:9, 65°C, pH 11) formed stable nanoparticles (Z-average 63–81 nm) while Nisin-SNPs formed larger conjugates yet exhibited markedly enhanced antibacterial activity compared to nisin alone. Results indicate that SNP conjugation can enhance the antimicrobial potency of purified bacteriocins, but outcomes depend critically on peptide type, purity, and synthesis parameters. Further *in vivo* safety and mechanistic studies are warranted.

6. Acknowledgements

The authors gratefully acknowledge the funding and support provided by the Universiti Putra Malaysia (UPM) under Geran Putra Inisiatif (GPI/2024/9793600) and Geran Putra GP-IPS (GP-IPS/2025/9819800).

7. Author contributions

Noor Azman, INS.: Conceptualization, Data curation, Investigation, Methodology, Visualization, Writing – original draft; Wan Adnan, WAH.: Formal analysis, Investigation, Visualization; Paannerchelvan, S.: Writing – review & editing, Validation; Mohamad, R.: Conceptualization, Resources, Supervision; Abdul Rahman, N.: Conceptualization, Resources, Supervision; Wasoh, H.: Conceptualization, Resources, Supervision; Mohd Sobri, MZ.: Conceptualization, Resources; Halim, M.: Conceptualization, Funding acquisition, Project administration, Supervision, Validation, Writing – review & editing.

8. Conflict of interest

The authors declare that they have no conflict of interest.

9. References

[1] Bertagnolio S, Suthar AB, Tosas O, Van Weezenbeek K. Antimicrobial resistance: Strengthening surveillance for public health action. PLoS Med. 2023;20(7):e1004265.

[2] Li Y, Sheng Y, Weng P, Wu Z, Liu Y. Purification and antimicrobial mechanism of a novel bacteriocin produced by Lactiplantibacillus plantarum FB-2. LWT. 2023;185:115123.

[3] Darbandi A, Asadi A, Ari MM, Ohadi E, Talebi M, Zadeh MH, et al. Bacteriocins: Properties and potential use as antimicrobials. J Clin Lab Anal. 2022;36(1):e24093.

[4] Amer SA, Abushady HM, Refay RM, Mailam MA. Enhancement of the antibacterial potential of plantaricin by incorporation into silver nanoparticles. J Genet Eng Biotechnol. 2021;19(1):13.

[5] More PR, Pandit S, De Filippis A, Franci G, Mijaković I, Galdiero M. Silver nanoparticles: Bactericidal and mechanistic approach against drug resistant pathogens. Microorganisms. 2023;11(2):369.

[6] Sidhu PK, Nehra K. Bacteriocin-capped silver nanoparticles for enhanced antimicrobial efficacy against food pathogens. IET Nanobiotechnol. 2020;14(3):245-252.

[7] Aguilar-Garay R, Lara-Ortiz LF, Campos-López M, Gonzalez-Rodriguez DE, Gamboa-Lugo MM, Mendoza-Pérez JA, et al. A comprehensive review of silver and gold nanoparticles as effective antibacterial agents. Pharmaceuticals. 2024;17(9):1134.

[8] Yaqoob SB, Adnan R, Rameez Khan RM, Rashid M. Gold, silver, and palladium nanoparticles: A chemical tool for biomedical applications. Front Chem. 2020;8:376.

[9] Alzoubi FY, Ahmad AA, Ihsan AA, Migdadi AB, Al-Bataineh QM. Localize surface plasmon resonance of silver nanoparticles using Mie theory. J Mater Sci Mater Electron. 2023;34:2128.

[10] Lin G, Wu M, Tang R, Wu B, Wang Y, Zhu J, et al. A surface-enhanced Raman scattering substrate with tunable localized surface plasmon resonance absorption based on AgNPs. Sensors. 2024;24(17):5778.

[11] Kumar D, Kumar S, Gholap AD, Kumari R, Tanwar R, Kumar V, et al. A comprehensive review on the biomass-mediated synthesis of silver nanoparticles: Opportunities and challenges. J Environ Chem Eng. 2025;13(1):115133.

[12] Yazdi M, Yousefvand A, Hosseini HM, Mirhosseini SA. Green synthesis of silver nanoparticles using nisin and its antibacterial activity against Pseudomonas aeruginosa. Adv Biomed Res. 2022;11(1):56.

[13] Syame SM, Mansour AS, Khalaf DD, Ibrahim ES, Gaber ES. Green synthesis of silver nanoparticles using lactic acid bacteria: Assessment of antimicrobial activity. World Vet J. 2020;10(4):625-633.

[14] Sharma S, Sharma N, Kaushal N. Utilization of novel bacteriocin synthesized silver nanoparticles (AgNPs) for their application in antimicrobial packaging for preservation of tomato fruit. Front Sustain Food Syst. 2023;7:1072738.

[15] Youssef GA, Farag AM, Saad AH, El-Shenawy MA, El-Aassar S. Production, characterization and biosynthesis of silver nanoparticles bacteriocin of Lactobacillus sakei isolated from fish samples. Egypt J Aquat Biol Fish. 2022;26(4):135-155.

[16] Al-Hadede LT, Hassan MI. Silver nanoparticles synthesis by green method and loading of enterosein to study its antimicrobial inhibition. IOP Conf Ser Mater Sci Eng. 2020;928(7):072078.

[17] Akhter MS, Rahman MA, Ripon RK, Mubarak M, Akter M, Mahbub S, et al. A systematic review on green synthesis of silver nanoparticles using plant extract and their biomedical applications. Heliyon. 2024;10(11).

[18] Sidhu PK, Nehra K. Purification and characterization of bacteriocin Bac23 extracted from Lactobacillus plantarum PKLP5 and its interaction with silver nanoparticles for enhanced antimicrobial spectrum against food-borne pathogens. LWT. 2021;139:110546.

[19] Siddiqui AJ, Patel M, Adnan M, Jahan S, Saxena J, Alshahrani M, et al. Bacteriocin-nanoconjugates (Bac10307-AgNPs) biosynthesized from Lactobacillus acidophilus-derived bacteriocins exhibit enhanced and promising biological activities. Pharmaceutics. 2023;15(2):403.

[20] Dhaka A, Mali SC, Sharma S, Trivedi R. A review on biological synthesis of silver nanoparticles and their potential applications. Results Chem. 2023;6:101108.

[21] El-Zawawy NA, Abou-Zeid AM, Beltagy DM, Hantera NH, Nouh HS. Mycosynthesis of silver nanoparticles from endophytic Aspergillus flavipes AUMC 15772: Statistical optimization, characterization and biological activities. Microb Cell Fact. 2023;22(1):1-17.

[22] Mikhailova EO. Green silver nanoparticles: An antibacterial mechanism. Antibiotics. 2024;14(1):5.

[23] Singh P, Mijakovic I. Strong antimicrobial activity of silver nanoparticles obtained by green synthesis in Viridibacillus sp. extracts. Front Microbiol. 2022;13:820048.

[24] Jia Z, Li J, Gao L, Yang D, Kanaev A. Dynamic light scattering: A powerful tool for in situ nanoparticle sizing. Colloids Interfaces. 2023;7(1):15.

[25] Zimet P, Valadez R, Raffaelli S, Estevez MB, Pardo H, Alborés S. Biogenic silver nanoparticles conjugated with nisin: Improving the antimicrobial and antibiofilm properties of nanomaterials. Chemistry. 2021;3(4):1271-1285.

[26] Miranda A, Akpobolokemi T, Chung E, Ren G, Raimi-Abraham BT. pH alteration in plant-mediated green synthesis and its resultant impact on antimicrobial properties of silver nanoparticles (AgNPs). Antibiotics. 2022;11(11):1592.

[27] Bruna T, Maldonado-Bravo F, Jara P, Caro N. Silver nanoparticles and their antibacterial applications. Int J Mol Sci. 2021;22(13):7202.

[28] Fernando KM, Gunathilake CA, Yalegama C, Samarakoon UK, Fernando CAN, Weerasinghe G, et al. Synthesis of silver nanoparticles using green reducing agent: Ceylon olive (Elaeocarpus serratus): Characterization and investigating their antimicrobial properties. J Compos Sci. 2024;8(2):43.

[29] Qadi WSM, Mediani A, Kasim ZM, Misnan NM, Sani NA, Jamar NH. Biological characterization and metabolic variations among cell-free supernatants produced by selected plant-based lactic acid bacteria. Metabolites. 2023;13(7):849.

[30] Drumond MM, Tapia-Costa AP, Neumann E, Nunes ÁC, Barbosa JW, Kassuha DE, et al. Cell-free supernatant of probiotic bacteria exerted antibiofilm and antibacterial activities against Pseudomonas aeruginosa: A novel biotic therapy. Front Pharmacol. 2023;14:1152588.

[31] Kurnianto MA, Kusumaningrum HD, Lioe HN, Chasanah E. Partial purification and characterization of bacteriocin-like inhibitory substances produced by Streptomyces sp. isolated from the gut of Chanos chanos. Biomed Res Int. 2021;2021:7190152.

[32] Khelissa S, Chihib N, Gharsallaoui A. Conditions of nisin production by Lactococcus lactis subsp. lactis and its main uses as a food preservative. Arch Microbiol. 2020;203(2):465-480.

[33] Ryan A, Patel P, O'Connor PM, Ross RP, Hill C, Hudson SP. Pharmaceutical design of a delivery system for the bacteriocin lacticin 3147. Drug Deliv Transl Res. 2021;11(4):1735-1751.

[34] Dhanam S, Arumugam T, Elgorban AM, Rameshkumar N, Krishnan M, Govarthanan M, et al. Enhanced anti-methicillin-resistant Staphylococcus aureus activity of bacteriocin by encapsulation on silver nanoparticles. Appl Nanosci. 2023;13(2):1301-1312.